Supporting Information

Pt^{II}_6 Nanoscopic cages with organometallic backbone as sensors for picric acid

Dipak Samanta and Partha Sarathi Mukherjee*

[†]*Department of Inorganic and Physical Chemistry, Indian Institute of Science, Bangalore-560 012, India. Fax: 91-80-2360-1552; Tel; 91-80-2293-3352*

E-mail: psm@ipc.iisc.ernet.in

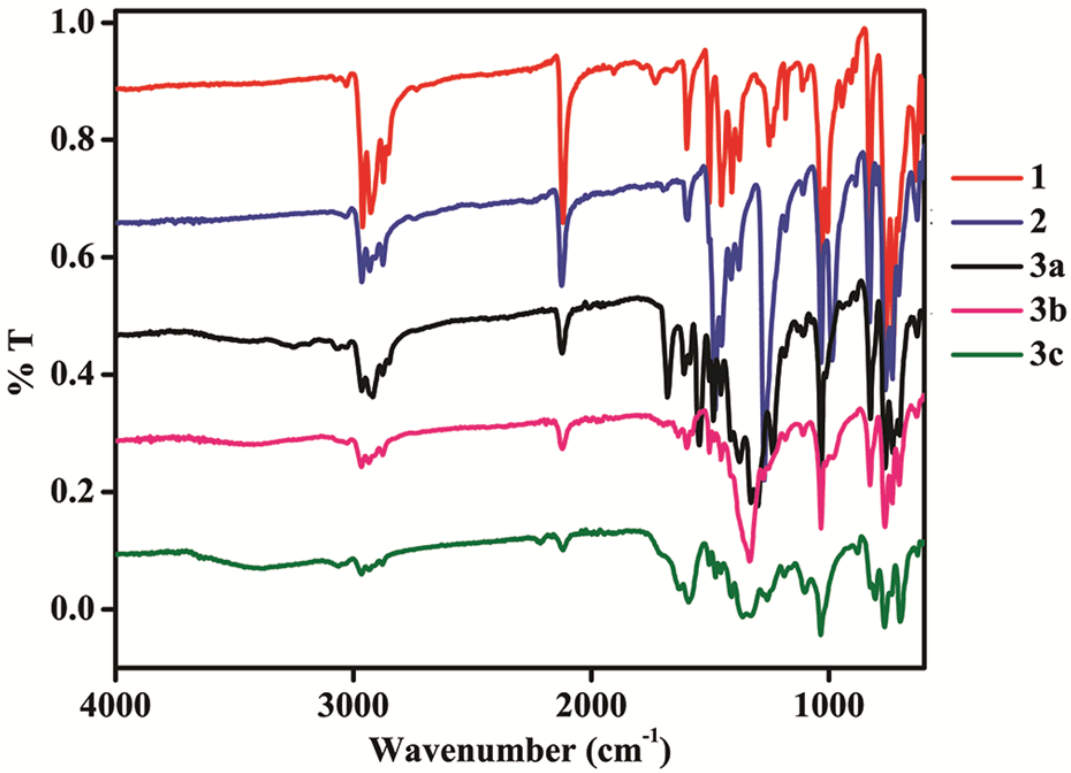

Fig. S1 IR spectra of the complexes **1**, **2** and prisms **3a** – **3c**.

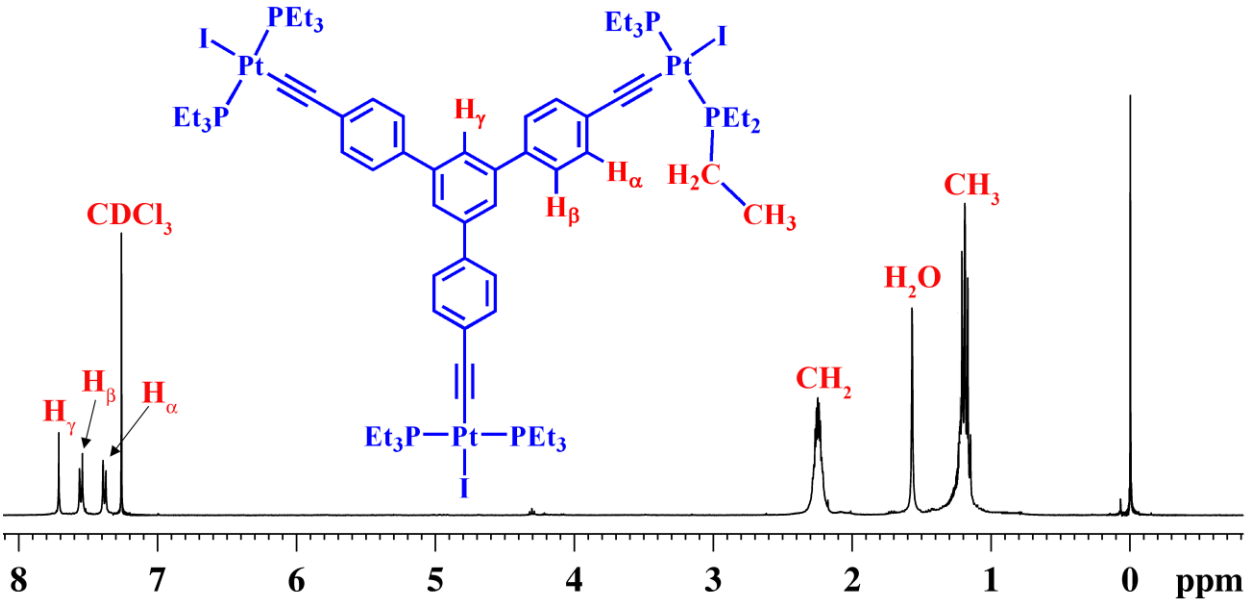

Fig. S2 ^{1}H NMR spectrum of complex **1** recorded in $CDCl_3$.

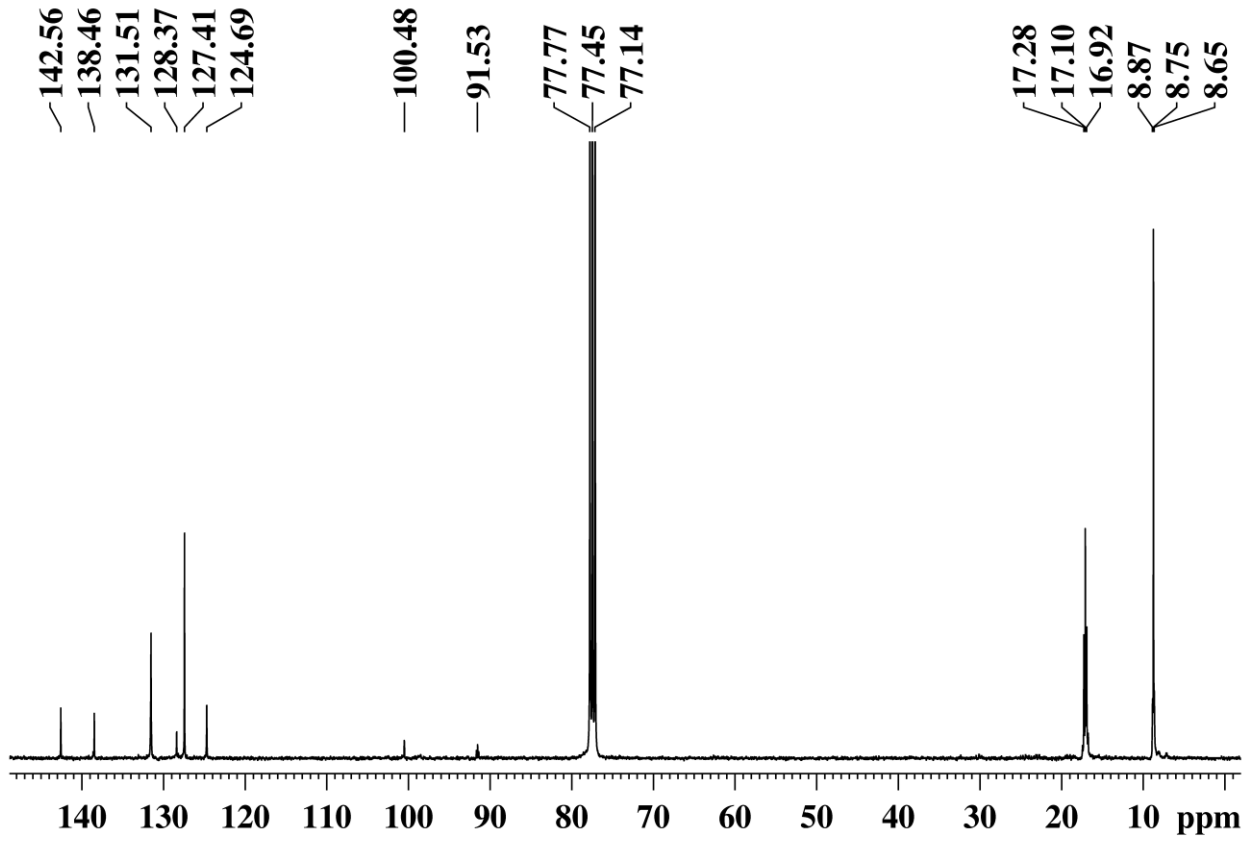

Fig. S3 ^{13}C NMR spectrum of complex **1** recorded in $CDCl_3$.

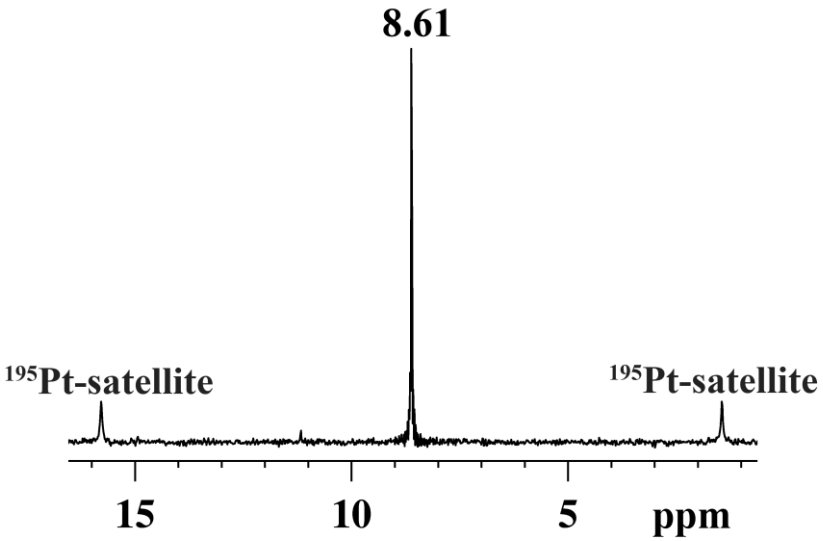

Fig. S4 ^{31}P NMR spectrum of complex **1** recorded in $CDCl_3$.

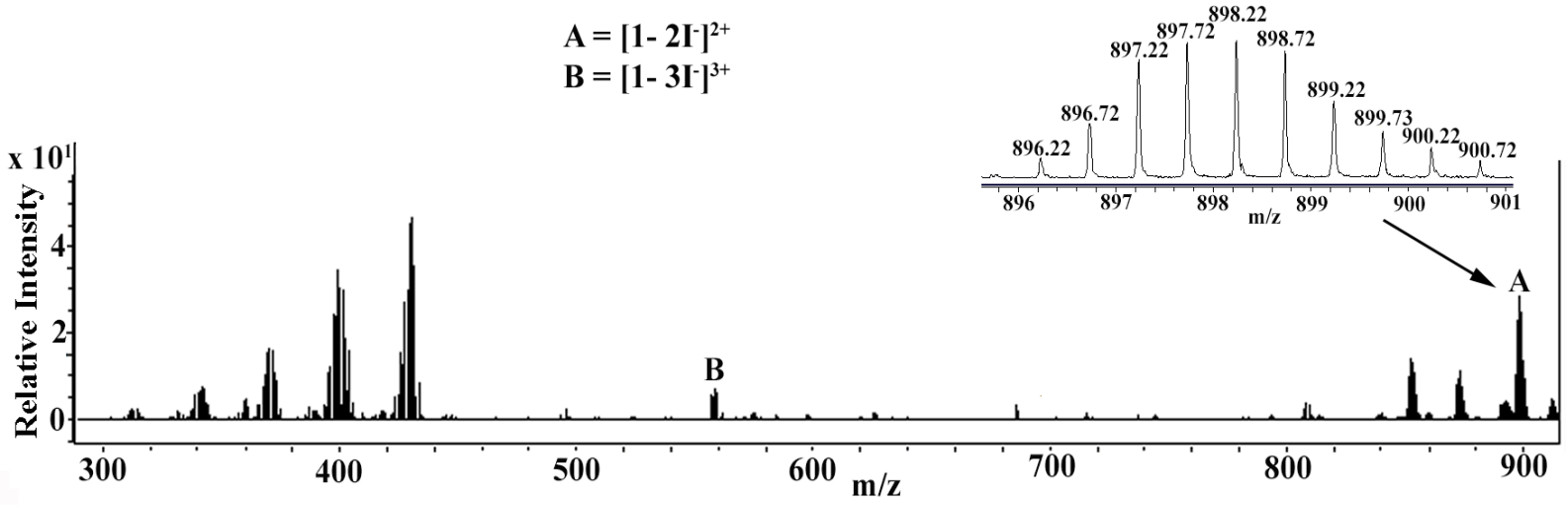

Fig. S5 ESI-MS spectrum of the **1** recorded in CH_3CN and $CHCl_3$ mixture. Inset: Experimentally detected isotopic distribution of the fragment $[\mathbf{1} - 2I^-]^{2+}$.

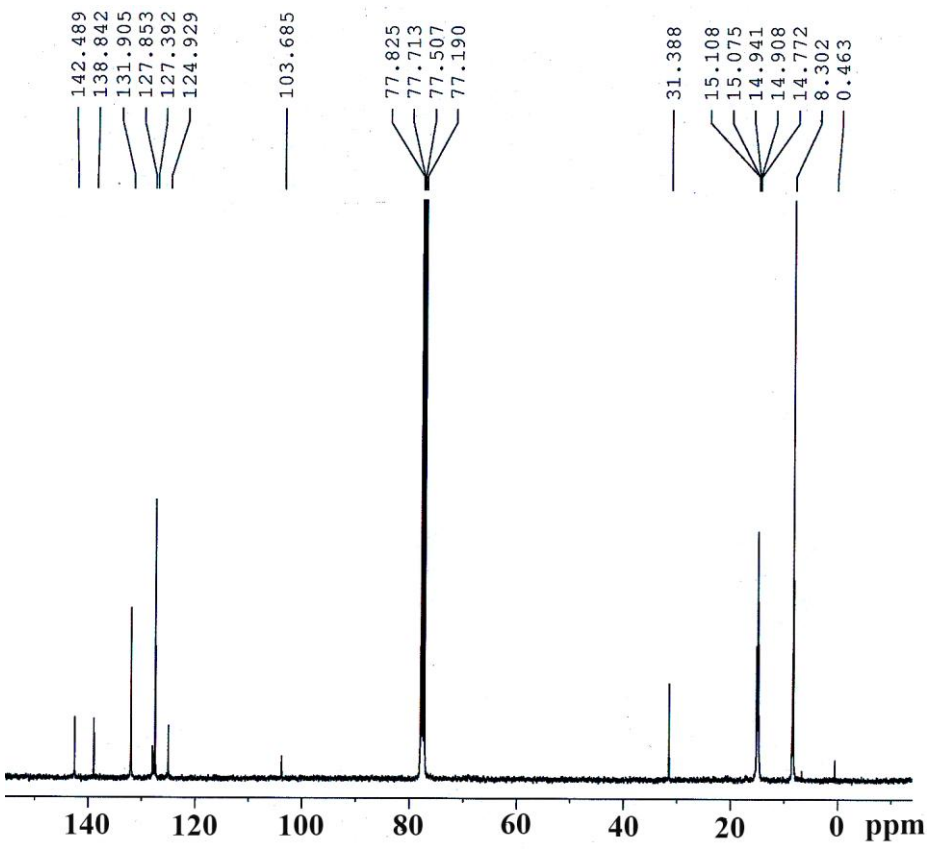

Fig. S6 ^{13}C NMR spectrum of complex **2** recorded in $CDCl_3$.

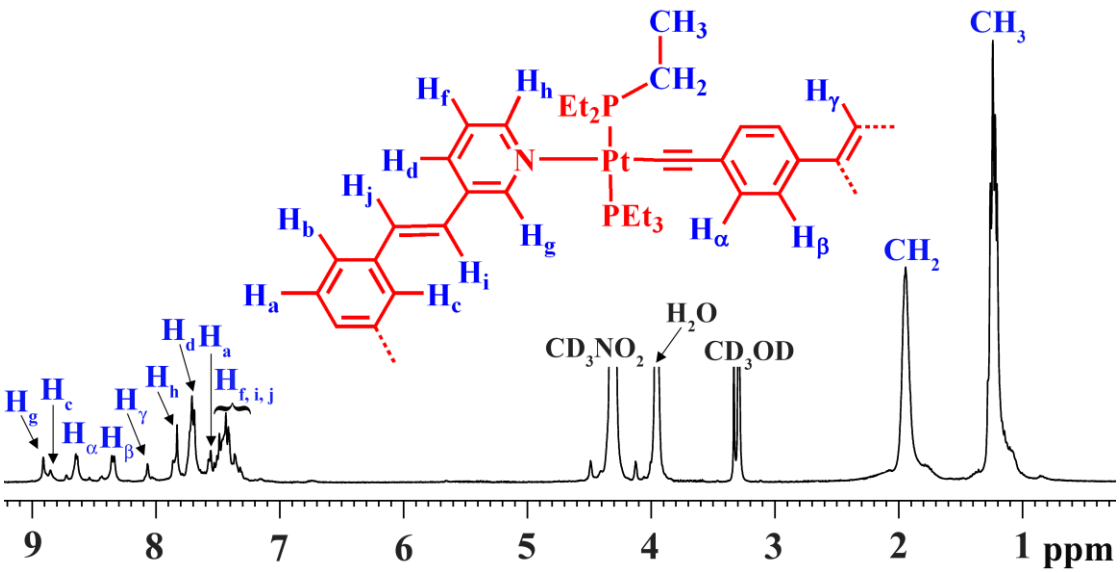

Fig. S7 ^{1}H NMR spectrum of the macrocycle **3b** recorded in CD_3NO_2 and CD_3OD mixture.

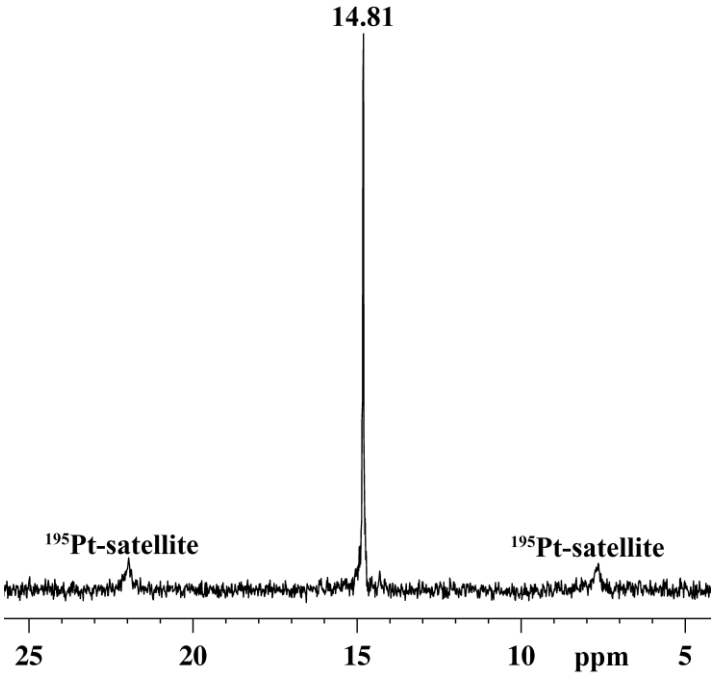

Fig. S8 ^{31}P NMR spectrum of the macrocycle **3b** recorded in CD_3NO_2 and CD_3OD mixture.

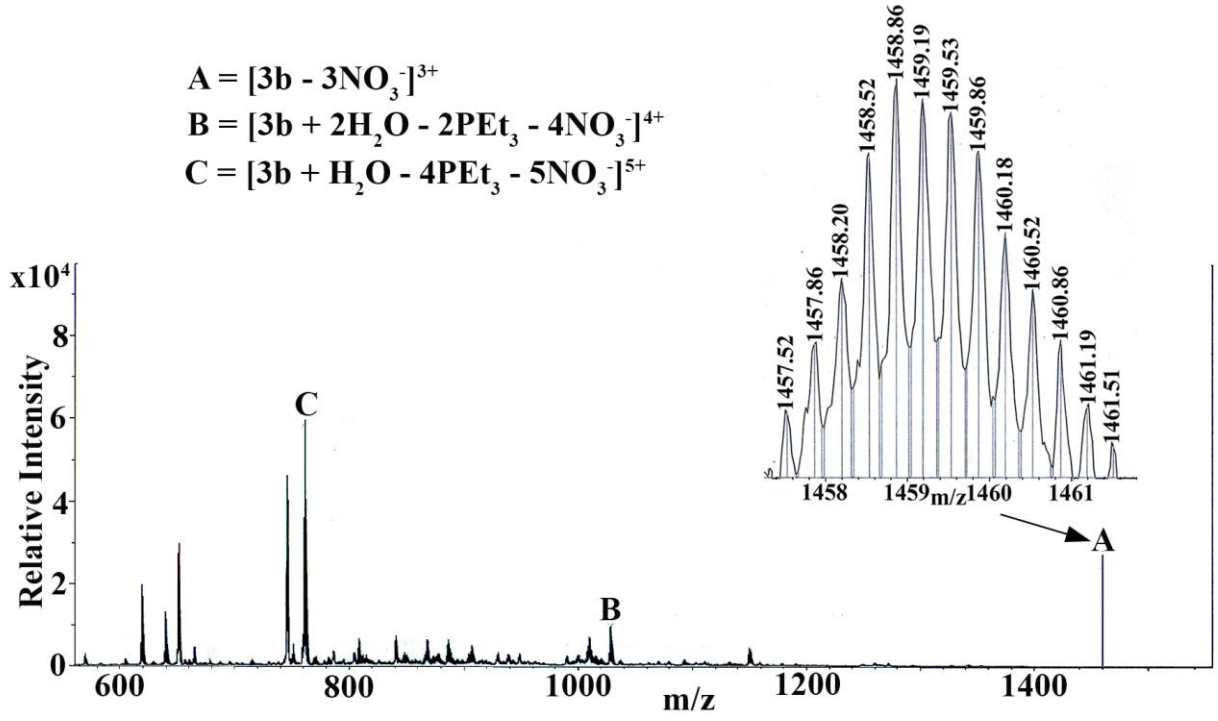

Fig. S9 ESI-MS spectrum of the macrocycle **3b** recorded in CH_3CN. Inset: Experimentally detected isotopic distribution of the fragment [**3b** – $3NO_3^-$]$^{3+}$.

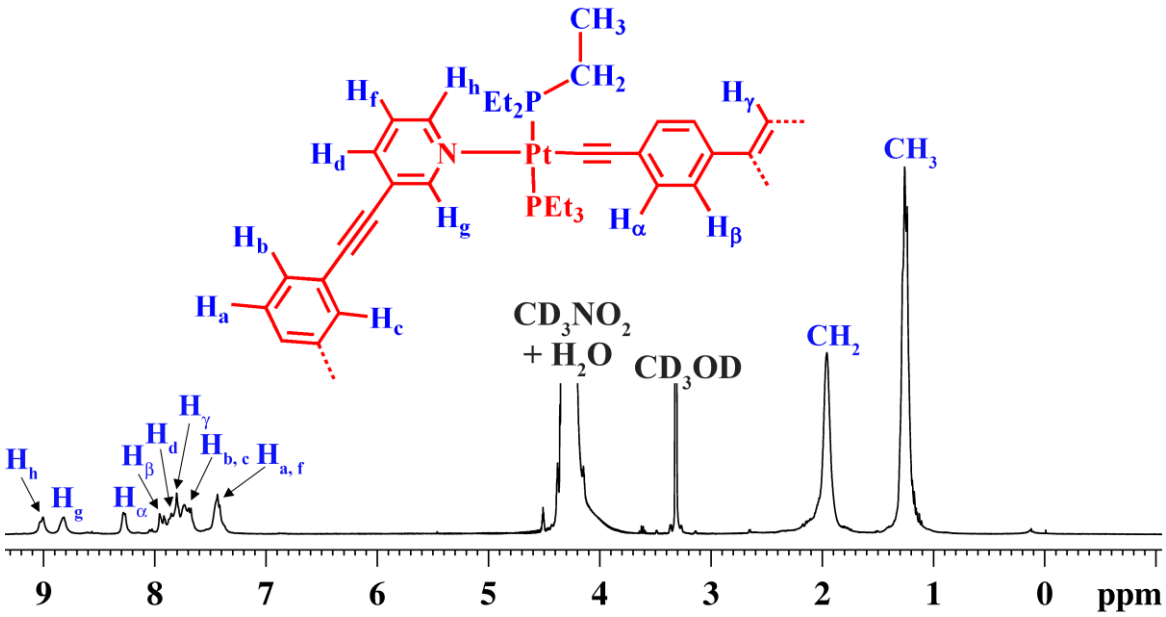

Fig. S10 ^{1}H NMR spectrum of the macrocycle **3c** recorded in CD_3NO_2 and CD_3OD mixture.

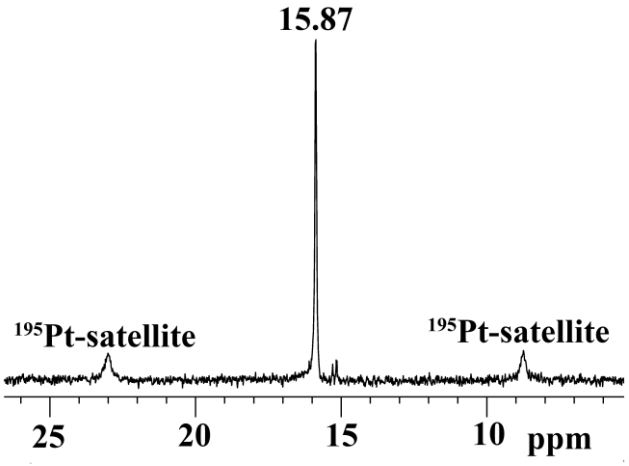

Fig. S11 ^{31}P NMR spectrum of the macrocycle **3c** recorded in CD_3NO_2 and CD_3OD mixture.

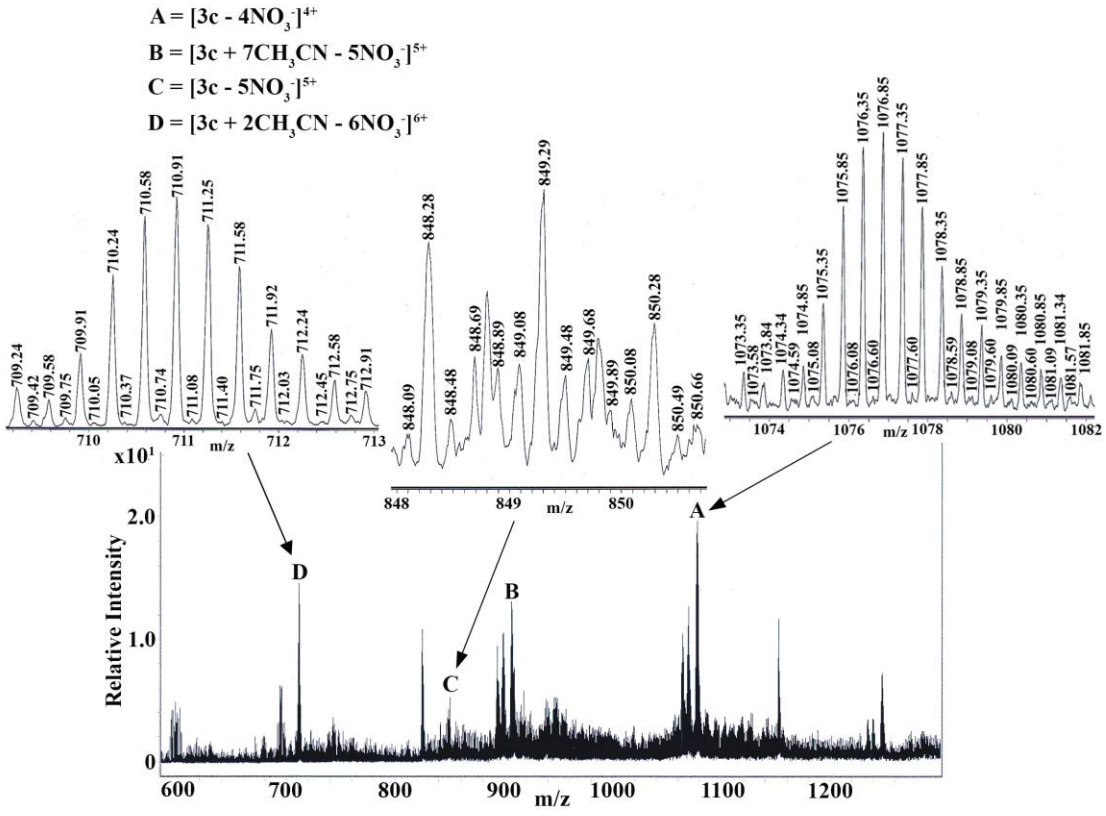

Fig. S12 ESI-MS spectrum of the macrocycle **3c** recorded in CH_3CN. Inset: Experimentally determined isotopic distributions of the fragments $[\mathbf{3c} - 4NO_3^-]^{4+}$. $[\mathbf{3c} - 5NO_3^-]^{5+}$, $[\mathbf{3c} + 2CH_3CN - 6NO_3^-]^{6+}$.

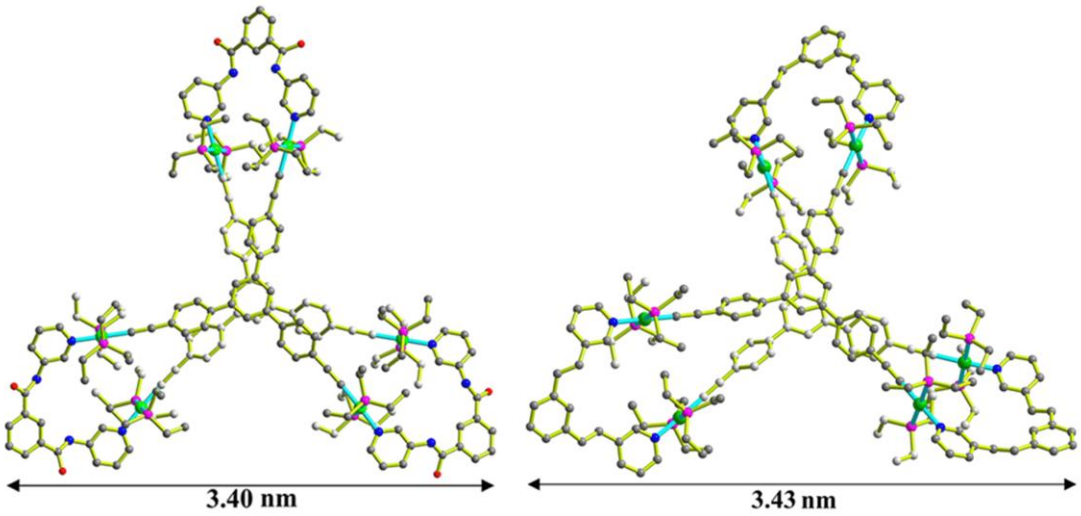

Fig. S13 Energy minimized structures of the prisms **3a** (left) and **3b** (right) (Color codes: green = Pt, magenta = P, blue = N, grey = C, red = O). The hydrogen atoms are omitted for clarity.

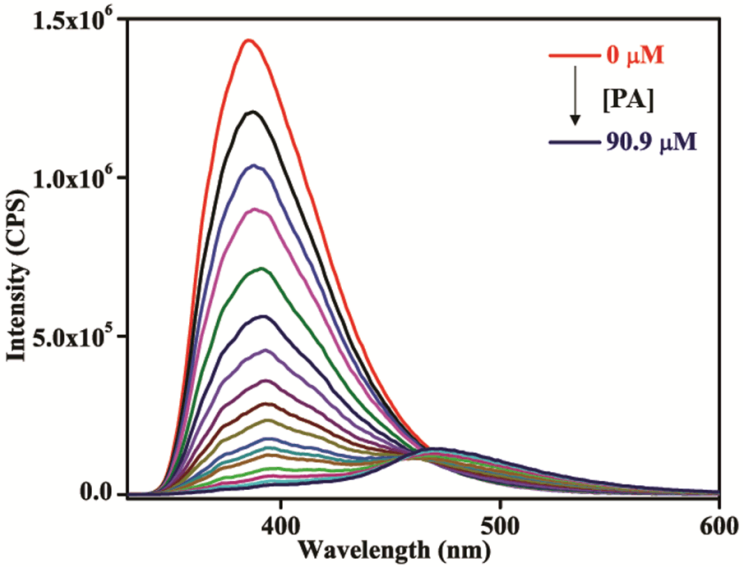

Fig. S14 Gradual reduction of emission intensity of acetonitrile solution (1.0×10^{-5} M) of **3b** upon addition of picric acid solution in chloroform (1.0×10^{-3} M).

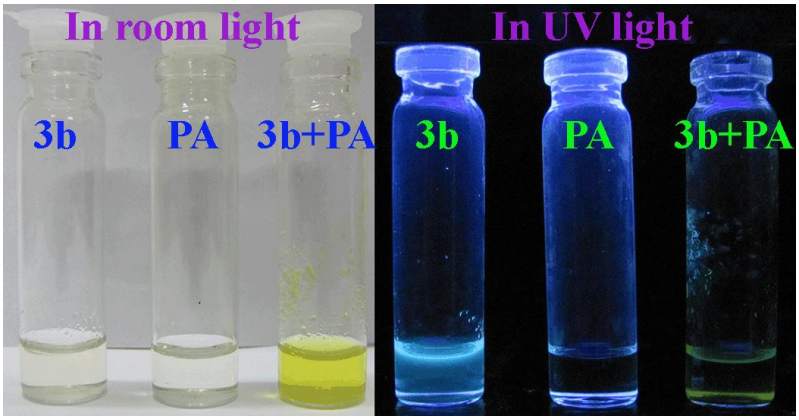

Fig. S15 Change of salient visual color upon exposing of acetonitrile solution of **3b** to chloroform solution of picric acid.

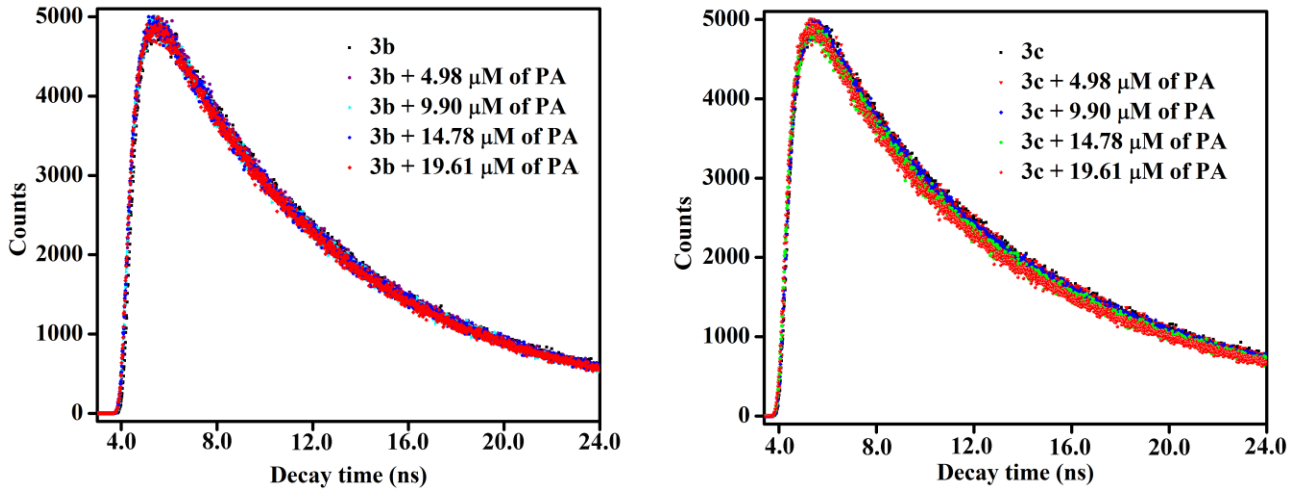

Fig. S16 Excited-state lifetime analysis by time-resolved fluorescence titration of acetonitrile solutions (1.0×10^{-5} M) of **3b** (left) and **3c** (right) with respect to increasing concentration of picric acid in chloroform (1.0×10^{-3} M).

Proof of ground state complex formation by ^{1}H NMR titration:

To confirm ground state complex formation, ^{1}H NMR experiments were performed with the addition of $CDCl_3$ solution (0.2 mL) of picric acid to a solution of **3b** /**3c** in CD_3CN (0.4 mL) at 4:1 molar ratio, separately. Substantial upfield shift in proton signal was observed in case of picric acid which is basically due to complex formation. The proton signal of picric acid was downfield shifted gradually with concomitant progress of dilution of the samples with 0.2 mL of $CDCl_3$ each time (Fig. S17, Supporting Information), but the peaks corresponding to the macrocycles showed almost no shift. The detected downfield shifting of proton resonance of the picric acid upon dilution is presumably, due to, shifting of equilibrium position from charge-transfer complex to the isolated picric acid state. Lifetime analysis, absorption spectra and ^{1}H NMR titration with observed visual color change indicate the formation of ground state charge-transfer complex.

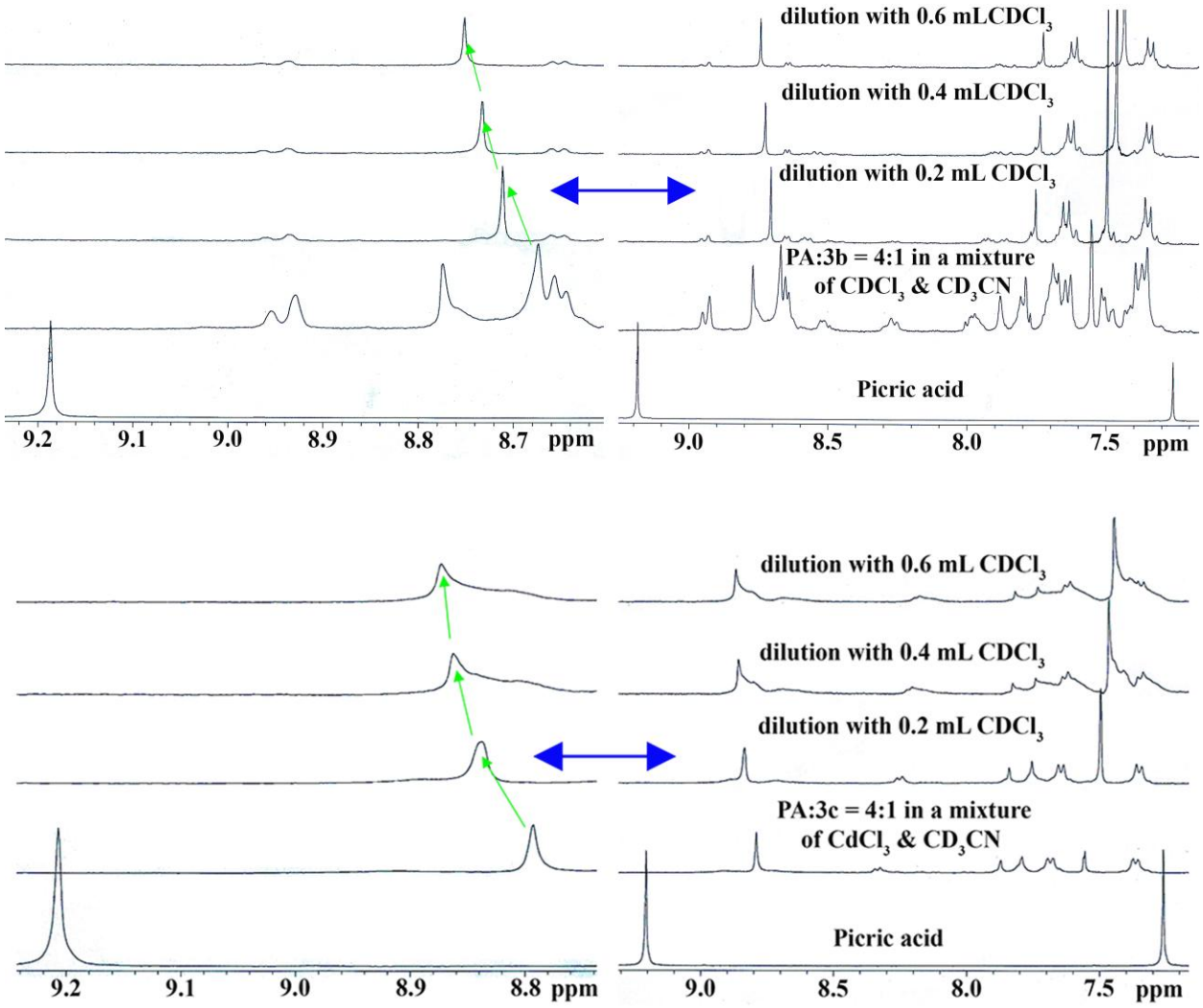

Fig. S17 ^{1}H NMR spectra of a solution of picric acid and **3b** (top) or **3c** (bottom) in 4:1 molar ratio in $CDCl_3$ and CD_3CN upon subsequent dilution with 0.2 mL of $CDCl_3$ each time.

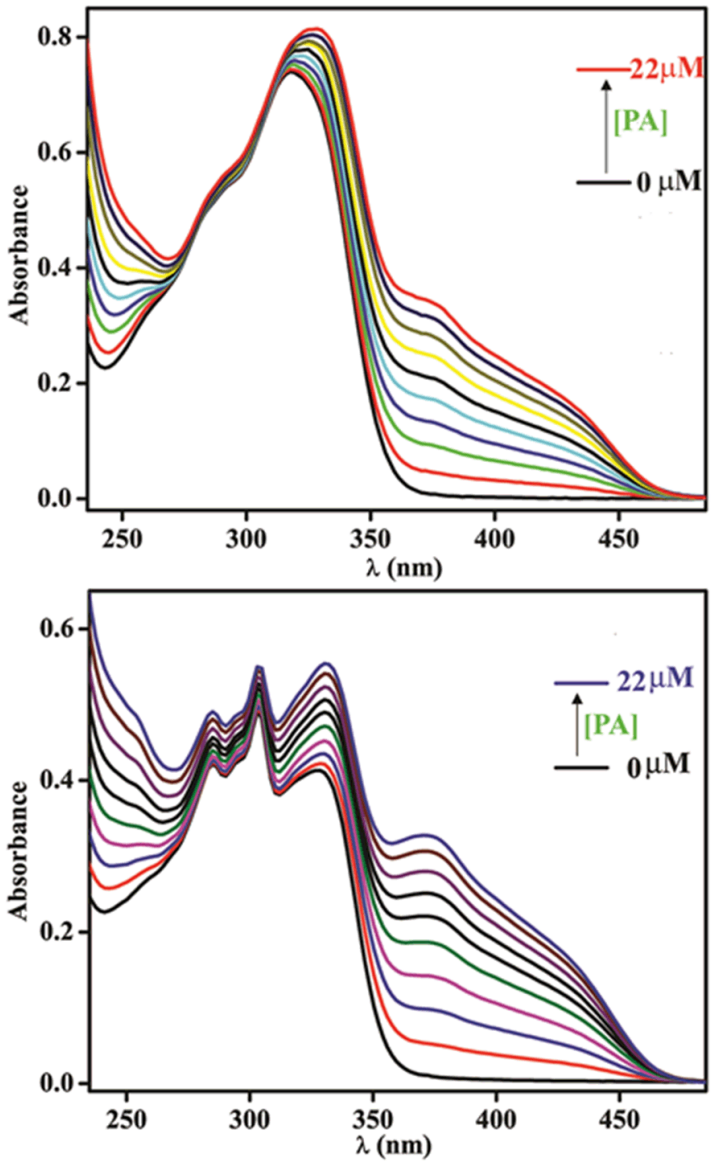

Fig. S18 Change in absorption spectra of the macrocycles **3b** (top) and **3c** (bottom) in CH_3CN (2.5×10^{-6} M) upon gradual addition of picric acid in chloroform ($0 – 22 \times 10^{-6}$ M) at 25°C.

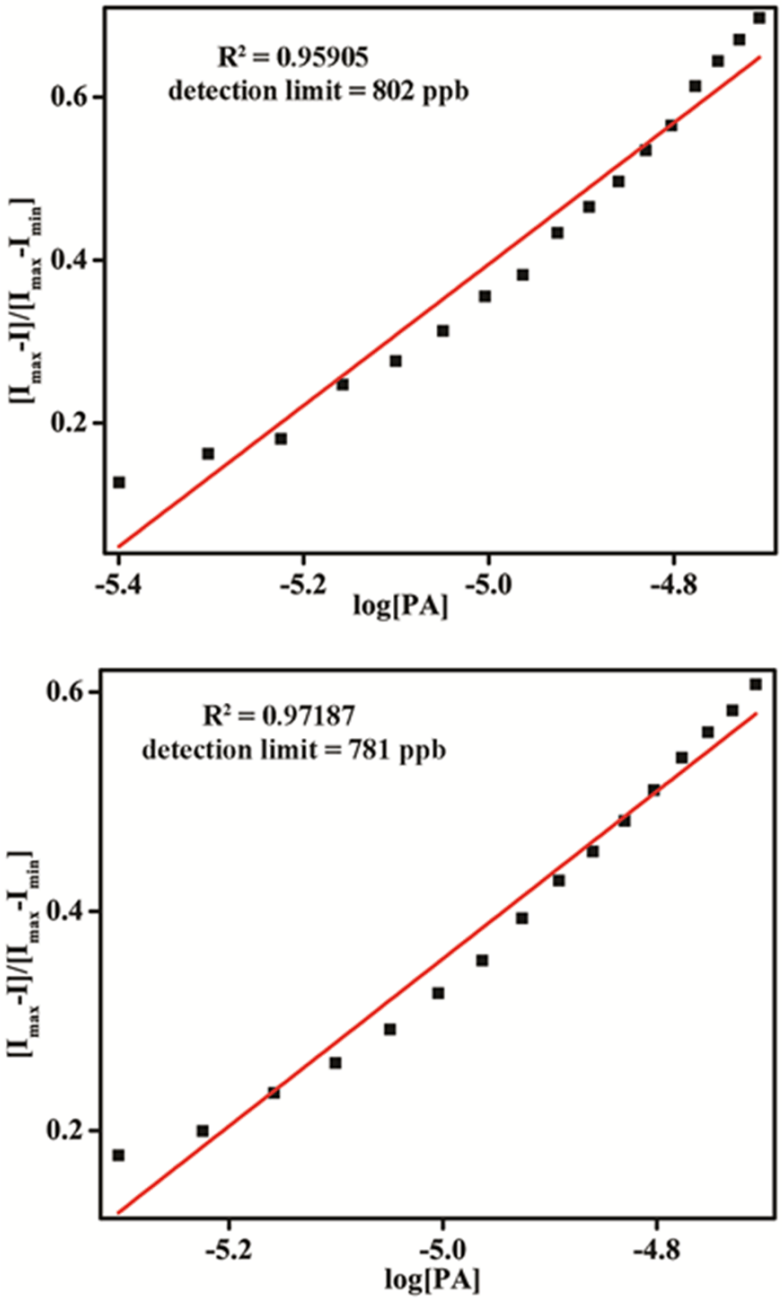

Fig. S19 **(**I_{max}-I)/(I_{max}-I_{min}) vs log[PA] plots for **3b** (top) and **3c** (bottom). The calculated detection limits (obtained from the intercepts of the plots on X-axis) are 3.5×10^{-6} μL (**3b**) and 3.4×10^{-6} μL (**3c**).